

Quantum Chemical Studies of Pyrophosphate Hydrolysis

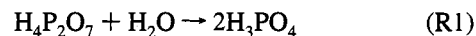
Michael E. Colvin,^{*,†} Earl Evleth,[‡] and Yamina Akacem[‡]*Contribution from the Center for Computational Engineering, Department 8117 Sandia National Laboratories, Livermore, California 94551-0969, and Laboratoire de Dynamique des interactions Moléculaires, ER 271, Université Pierre et Marie Curie, 4 Place Jussieu, 75230 Paris, France*Received April 11, 1994[®]

Abstract: The hydrolysis of pyrophosphate to form two orthophosphates is coupled to virtually all biosynthetic reactions. Despite numerous experiments, a detailed understanding of the energetic factors contributing to this reaction energy is still lacking. In this paper we describe large basis set *ab initio* calculations of the reaction energy for pyrophosphate hydrolysis. These calculations were performed using second-order Møller–Plesset perturbation theory at the Hartree–Fock/6-311++G** optimized geometries. We find that in the gas phase the hydrolysis of the fully-protonated pyrophosphate is disfavored by 5 kcal/mol. The origin of this unfavorable free energy is a pair of intramolecular hydrogen bonds that link the two phosphate moieties. For the anionic forms of pyrophosphate that exist near neutral pH, the gas-phase hydrolysis energies are strongly negative due to electrostatic repulsion. We have also predicted the aqueous phase hydration energy using several methods based on a dielectric continuum model of the aqueous solvent. Aqueous solvation acts to cancel this repulsion; the *ab initio* aqueous phase result, which we expect to be most reliable, predicts hydrolysis energies of 3 to 7 kcal/mol for the protonation states predominant near physiological pH.

Introduction

The hydrolysis of pyrophosphate to form two orthophosphates is coupled to virtually all biosynthetic reactions. In many cases, such as the synthesis of polynucleotides, this hydrolysis determines the direction of the reaction. Numerous measurements have indicated that the reaction free energy of inorganic pyrophosphate hydrolysis is approximately -5 kcal/mol. However, despite these empirical results, a detailed understanding of the energetic factors contributing to this reaction energy is still lacking. In particular, it is unknown to what extent this reaction energy is determined by intermolecular versus intramolecular effects. The high-energy phosphate bond was originally thought due to intramolecular effects ranging from simple electrostatic repulsion to more complex “opposing resonance” effects. This hypothesis was challenged by George *et al.*,¹ who found that the reaction enthalpy for pyrophosphate hydrolysis was *inversely* related to the total charge of the phosphates with $\Delta H^\circ = 7.6$ kcal/mol for the hydrolysis of $H_4P_2O_7$ and $\Delta H^\circ = -3.7$ kcal/mol for the hydrolysis of $P_2O_7^{4-}$, exactly the opposite of that expected if electrostatic repulsion was dominating the reaction energetics. Experiments on the hydrolysis reaction in nonpolar solvents suggest that the negative reaction energy may be entirely a result of differing solvation energies of the reactant and products. Romero² determined that for pyrophosphate hydrolysis, $\Delta G^\circ = -5.1$ kcal/mol in H_2O , -1.6 kcal/mol in 50% Me_2SO , and $+0.1$ kcal/mol in 50% poly(ethylene glycol). It should be noted the experimental results are not unambiguous; recent data for the hydrolysis of adenosine 5'-triphosphate³ indicates that the reaction enthalpy increases from -13.1 kcal/mol at pH 6.4 to -16.3 kcal/mol at pH 8.8, the opposite of the trend found for pyrophosphate hydrolysis.

Pyrophosphate hydrolysis is a particularly difficult problem for *ab initio* studies because the reactants and products are multiply deprotonated at neutral pH. To date, most predictions of the reaction enthalpy have been for the fully protonated “gas-phase” reaction:



with the goal of establishing whether the unsolvated reaction is endothermic or exothermic. These studies have not unambiguously resolved this issue, predicting a wide range of gas-phase hydrolysis enthalpies ranging from -0.4 to -13.4 kcal/mol.^{4–7}

In this paper we describe large basis set *ab initio* calculations of the gas-phase reaction enthalpy and free energy of pyrophosphate hydrolysis. These calculations were performed on the fully protonated states of the pyrophosphate reactants and the phosphate products using second-order Møller–Plesset perturbation theory at the Hartree–Fock/6-311++G** optimized geometries. Additionally, we have predicted the hydrolysis energies for the deprotonated states of pyrophosphates using several methods based on a dielectric continuum model of the aqueous solvent to estimate solvation energies of the reactants and products. Finally, a comparison of the *ab initio* and semiempirical results will be made in order to evaluate their relative performance.

Methods

The molecular structures of all protonation states of pyrophosphate and orthophosphate were optimized within the Hartree–Fock approximation using both a 6-31G* and a larger 6-311++G** basis set. Single-point second-order Møller–Plesset perturbation theory energy calculations (with the core electrons frozen) were performed using both basis sets at the HF/6-31G* and HF/6-311++G** optimized

[†] Sandia National Laboratories.

[‡] Université Pierre et Marie Curie.

[®] Abstract published in *Advance ACS Abstracts*, April 1, 1995.

(1) George, P.; Witonsky, R. J.; Trachtman, M.; Wu, C.; Dorwart, W.; Richman, L.; Richman, W.; Shurayh, F.; Lentz, B. *Biochim. Biophys. Acta* **1970**, *223*, 1.

(2) Romero, P. J.; de Meis, L. *J. Biol. Chem.* **1989**, *264*, 7869.

(3) Gajewski, E.; Steckler, D. K.; Goldberg, R. N. *J. Biol. Chem.* **1986**, *261*, 12733.

(4) Hayes, D. M.; Kenyon, G. L.; Kollman, P. A. *J. Am. Chem. Soc.* **1978**, *100*, 4331.

(5) O'Keefe, M.; Domenges, B.; Gibbs, G. V. *J. Phys. Chem.* **1985**, *89*, 2304.

(6) Ewig, C. S.; Van Waser, J. R. *J. Am. Chem. Soc.* **1988**, *110*, 79.

(7) Saint-Martin, H.; Otega-Blake, I.; Lez, A.; Adamowitz, L. *Biochim. Biophys. Acta* **1991**, *1080*, 205.

geometries. Additionally, the entropy of formation of each species was estimated using standard thermodynamic approximations.⁸ All *ab initio* calculations were performed using Gaussian 92.⁹

In order to model solvation effects and to calculate accurately atomic charge distributions, we have used several theoretical methods based on the polarizable continuum model for solvents. The first of these is a first-principles method developed independently by Miertus and Tomasi¹⁰ and Rashin.¹¹ This method is described in detail elsewhere, so only a brief description is given here.¹² The surrounding medium is treated as a continuum dielectric in a procedure involving several steps. First, the molecular geometry and electronic wave function are obtained from the Hartree-Fock calculation. Next, the interface between the molecule and the dielectric continuum of the surrounding medium is defined by the contact surface of the solvent molecule rolling around the scaled Van der Waal's surface of the molecule. The boundary-element method is used to represent the triangulated surface, as developed by Zauhar and Morgan.¹³ The electric potential is used to determine effective atomic charges (using a least-squares fit with constraints for net charge and dipole moments). Applying Gauss's law, the resulting electric field at the molecule surface (obtained from the atomic charges) is used to determine the effective charge of the dielectric continuum at the surface. These induced charges at the surface are then included in the one-electron portion of the HF Hamiltonian and the wave function is reoptimized. New atomic charges are calculated from the reoptimized wave function and the whole procedure is iterated to convergence (typically 8 iterations). A single-point MP2 energy calculation including the converged image charges is used to determine the total solvated energy. The surface area and volume of the molecule are used in an approximate expression¹⁴ to determine the free energy of cavitation (the non-electrostatic energy to create a cavity in the dielectric continuum containing the molecule). The theoretical free energy of solvation is the sum of the free energy of hydration (calculated as the difference between the *in vacuo* and solvated MP2 energies) and the free energy of cavitation. Note that an additional term of 1.84 kcal/mol is added for the work required to compress the solute from the standard gas-phase volume of 22.4 L to the standard aqueous-phase volume of 1 L.

A study of the performance of this model¹² indicates that it predicts absolute ΔG_{solv} 's accurate to 5 kcal/mol for several neutral, ionic, and zwitterionic compounds. Larger errors of up to 11 kcal/mol occur for small nonpolar molecules such as neutral trimethylamine where ΔG_{solv} is not dominated by electrostatic solute-solvent interactions. For these compounds, dispersion and solvent reorganization energies, not included in these predictions, act to cancel out the cavitation energy.

In addition to this non-empirical method, we applied the AM1-SM2 and PM3-SM3 methods of Cramer and Truhlar¹⁵ to all pyro- and orthophosphate species. By inclusion of empirical corrections and by allowing structural relaxation of the molecule, they have predicted solvation energies to within 1 kcal/mol for a wide range of neutral molecules. However, since these methods are based on semiempirical electronic wave functions, there is some question as to how accurately it will perform on second-row atoms.¹⁶ These calculations were

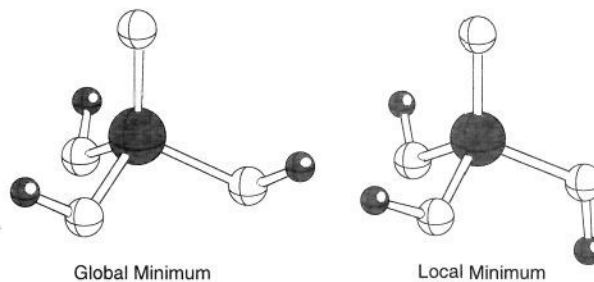


Figure 1. HF/6-311++G** optimized structures for H_3PO_4 . C_{3v} global minimum shown at left; C_1 symmetry local minimum 0.7 kcal/mol higher in energy shown at right.

performed with AMPAC 4.5.¹⁷ Note that for all the solvation energy calculations, the standard states are 1 mol/L in both the gas and condensed phases.

Results

The 6-311++G** HF optimized internal coordinates are given in Z-matrix form in Table S1 (supplementary material). The torsional potential energy surfaces of all hydroxyl groups were searched to find the global minimum energy configurations. (The torsional potential energy surfaces of the ortho- and pyrophosphate hydroxyls are shown in Figures S1 and S2, supplementary materials.) All of these structures were determined to be true minima on the potential energy surface by the calculation of analytic HF second derivatives at these optimized geometries. The *ab initio* total molecular energies, zero-point vibrational enthalpies, and total entropies are listed in supplementary material Table S2. The semiempirical, AM1 and PM3 enthalpies, entropies, and zero-point energies are given in supplementary material Table S3. The results for the boundary-element polarizable continuum method (PCM/*ab initio*) for all phosphates studied are given in Table 4. The total solvation energies from the polarizable continuum, AM1-SM2, and PM3-SM3 methods are given in Table 5.

Discussion

(I) Gas-Phase Results. (a) Neutral Species. The structure predicted for the orthophosphate is in very good agreement with structures predicted in earlier studies.⁷ The global minimum has C_{3v} symmetry with all three hydrogens above the plane of the hydroxy oxygens (see Figure 1). The effect of the basis set on the predicted neutral orthophosphate structure is minimal. The HF/6-311++G** P=O bond length is 1.446 Å and the P-O bond length is 1.571 Å, versus 1.453 and 1.571 Å by Saint-Martin⁷ using a 6-31G* basis set with polarization functions on P only.

The situation is more complicated for $\text{H}_4\text{P}_2\text{O}_7$ for which there is widespread disagreement about the optimal configuration. Our no-symmetry HF/6-31G* and HF/6-311++G** optimizations of pyrophosphate yielded a C_2 symmetry structure with the two intramolecular P-O...H-O hydrogen bonds linking opposite ends of the pyrophosphate. The optimized $\text{H}_4\text{P}_2\text{O}_7$ determined in this work is shown in Figure 2 compared with the optimized structure of Saint-Martin.⁷ Our $\text{H}_4\text{P}_2\text{O}_7$ structure differs from that of Saint-Martin (and all earlier structures) primarily by the presence of the hydrogen bonds. Interestingly, Ewig and Van Wazer⁶ found a very similar optimal conformation for disphosphonic acid ($\text{H}_4\text{P}_2\text{O}_5$) but did not find any intramolecular hydrogen bonds for pyrophosphate.

(17) AMPAC 4.5, Semichem, Inc.: 12715 West 66th Terrace, Shawnee, KS 66216.

(8) Hout, R. F., Jr.; Levi, B. A.; Hehre, W. J. *J. Comput. Chem.* **1982**, *3*, 234.

(9) Gaussian 92: Frisch, M. J.; Trucks, G. W.; Head-Gordon, M.; Gill, P. M. W.; Wong, M. W.; Foresman, J. B.; Johnson, B. G.; Schlegel, H. B.; Robb, M. A.; Replogle, E. S.; Gomperts, R.; Andres, J. L.; Raghavachari, K.; Binkley, J. S.; Gonzalez, C.; Martin, R. L.; Fox, D. J.; Defrees, D. J.; Baker, J.; Stewart, J. J. P.; Pople, J. A.; Gaussian Inc.: Pittsburg, 1992.

(10) Miertus, S.; Scrocco, E.; Tomasi, J. *Chem. Phys.* **1981**, *55*, 117.

(11) Rashin, A. A.; Namboodiri, K. *J. Phys. Chem.* **1987**, *91*, 6003.

(12) Colvin, M. E.; Melius, C. F. *Continuum Solvent Models for Computational Chemistry*; Sandia National Laboratories Technical Report SAND93-8239, 1993 (available from author or National Technology Information Service, U.S. Department of Commerce, 5285 Port Royal Rd., Springfield, VA 22161).

(13) Zauhar, R. J.; Morgan, R. S. *J. Mol. Biol.* **1985**, *186*, 815.

(14) Halicioglu, T.; Sinanoglu, O. *Ann. N.Y. Acad. Sci.* **1969**, *158*, 308.

(15) Cramer, C. J.; Truhlar, D. G. *J. Comput.-Aided Mol. Des.* **1992**, *6*, 629.

(16) Evleth, E.; Akacem, Y.; Colvin, M. E. *Chem. Phys. Lett.* **1994**, *227*, 412.

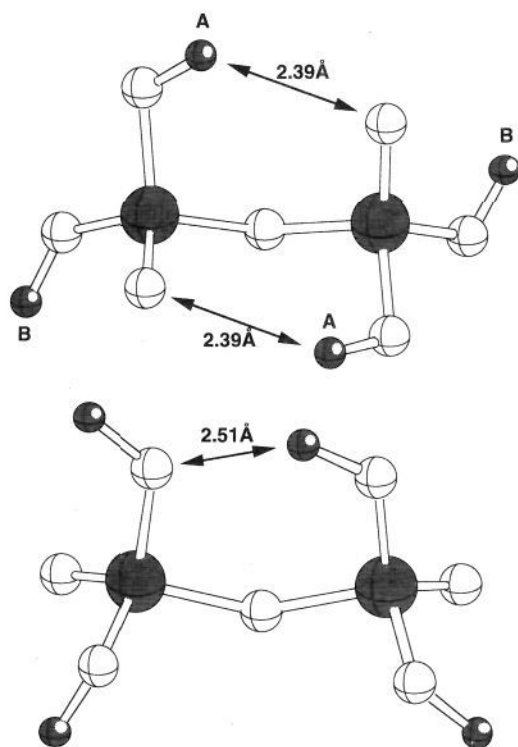


Figure 2. (a) $\text{H}_4\text{P}_2\text{O}_7$ Hartree-Fock/6-311++G** global minimum. The C2 symmetry structure has two symmetry distinct hydrogens labeled "A" and "B". Those labeled "A" are hydrogen bonded to the opposite phosphates. (b) Optimized structure from Saint-Martin.⁷ The major structural difference from the structure in part a is the lack of a pair of intramolecular hydrogen bonds. This structure possibly has a long H bond between the hydroxyls, but the H bond angle ($\angle\text{O}-\text{H}\cdots\text{O}$) is a very unfavorable 105° .

While there are no rigorous criteria defining hydrogen bonds ($\text{A}-\text{H}\cdots\text{B}$), they are usually characterized by the following properties: 3–10 kcal/mol interaction energies, $\text{H}\cdots\text{B}$ distances less than the sum of Van der Waals radii for H and B, a $\text{A}-\text{H}\cdots\text{B}$ bond angle within 20° of linear, and decreased A–H stretching frequencies.¹⁸ In our $\text{H}_4\text{P}_2\text{O}_7$ structure, the non-hydrogen-bonded hydroxyls (OH^{B} in Figure 2a) have torsional potential energy surfaces very similar to those of the hydroxyls in H_3PO_4 . In contrast, the H-bonding hydroxyls (OH^{A}) show a strong 8 kcal/mol orientation toward the oxygen on the opposite orthophosphate. (See supplementary material Figures S1 and S2). The length of the hydrogen bonds ($\text{H}\cdots\text{O}$) in our optimized structure is 2.39 Å, which is about 0.2 Å shorter than the sum of the conventional Van der Waals radii for hydrogen (1.2 Å) and oxygen (1.4 Å).¹⁹ Note that the configuration is not optimal for hydrogen bonding. The oxygen–oxygen distance of 3.06 Å is at the long end of the range found crystallographically, 2.60–3.05 Å, and the 127° $\text{O}-\text{H}\cdots\text{O}$ angle is outside the 160 – 180° range usually cited.²⁰

The HF/6-311++G** symmetric and antisymmetric harmonic stretching frequencies for the hydrogen-bonded $\text{O}-\text{H}^{\text{A}}$ are 4048 and 4052 cm^{-1} as compared to 4153 and 4151 cm^{-1} for $\text{O}-\text{H}^{\text{B}}$. These latter results are nearly identical to the $\text{O}-\text{H}$ stretching frequencies for the H_3PO_4 of 4164 cm^{-1} and (2) 4158 cm^{-1} indicating that the hydrogen bond has shifted the $\text{O}-\text{H}$ stretching frequency down by about 100 cm^{-1} which is commensurate with experimentally determined shifts for similar systems.¹⁸ The hydrogen bonding raises the $-\text{OH}$ torsional

(18) Vinogradov, S. N.; Lennell, R. H. *Hydrogen Bonding*; Van Nostrand Reinhold: New York, 1971.

Table 1. Gas Phase Hydrolysis Energies for Neutral Pyrophosphate (Reaction R1) (Note That the Enthalpies Include ZPE)

method	ΔH	ΔG
AM1	3.5	4.2
PM3	−2.0	−0.3
HF/6-31G**	0.0	−2.5
MP2/6-31G**	4.4	1.9
HF/6-311++G**	1.7	−0.9
MP2/6-311++G**	5.4	2.9

Table 2. Predicted Reaction Enthalpies for Pyrophosphate Hydrolysis (R1) from This and Earlier Work (kcal/mol)

authors, year	basis set and level of theory	published ΔH
this work, 1994	MP2/6-311++G**//HF/6-311++G**	+5.4
Saint-Martin, 1991	MP2/6-31G**//HF/6-31G* (D functions on P only)	−3.8
Ewig, 1988	HF/STO-3G*//HF/STO-3G*	(−3.3) ^a
O'Keefe, 1985	HF/6-31G//HF/3-21G	−0.4 ^b
Hayes, 1978	HF/4-31G/(partially opt.)	−5.5 ^b
		−13.2 ^b

^a MP2/6-311++G** enthalpy at Saint-Martin's geometry. ^b Does not include ZPE (+0.7 kcal/mol HF/6-311++G**).

rocking modes, which are shifted from 214 and 224 cm^{-1} for $-\text{OH}^{\text{B}}$ to 462 and 468 cm^{-1} for $-\text{OH}^{\text{A}}$.

The structure of the P–O–P bridge has been a source of some disagreement between the earlier *ab initio* studies. A wide range of bridging angles from 117° to 170° has been reported for differing basis sets. In particular, the presence of polarization functions on the bridging oxygen has a large effect on this angle. We predict a P–O–P angle of 118.4° from the HF/6-31G* optimization and 112.5° from the HF/6-311++G** optimization. The numbers are smaller than the most accurate published *ab initio* values of 139° ⁷ and 126° ⁶ as well as the crystal value of 133° .²¹ This difference can be attributed to the two intramolecular hydrogen bonds in our structure which act to reduce the P–O–P angle. Note also that this angle is extremely floppy (HF/6-311++G** harmonic bending frequency = 120 cm^{-1}) so that it will be highly dependent on intermolecular influences.

The gas-phase reaction energies for the hydrolysis reaction (R1) are given in Table 1. At the highest level of theory, we find the gas-phase hydrolysis enthalpy will be unfavorable by 5.4 kcal/mol. Including entropy we predict the free energy of the hydrolysis to be +2.9 kcal/mol. This result contradicts earlier published reaction enthalpies which are listed in Table 2. The most sophisticated calculations of these published results found the enthalpy of (R1) to be -3.8 kcal/mol at the MP2/6-31G**//RHF/6-31G* (D functions on P only) level of theory. The predicted reaction enthalpy using Saint-Martin's published $\text{H}_4\text{P}_2\text{O}_7$ structure, but recalculated at the MP2/6-311++G** level of theory, is -3.3 kcal/mol. These results clearly indicate that the differences in published reaction enthalpies are due to different optimized $\text{H}_4\text{P}_2\text{O}_7$ structures rather than differences in the calculation of the energy. In particular, the lack of intramolecular hydrogen bonding in the earlier structures destabilized the pyrophosphate relative to the orthophosphates. In our calculations, however, instead of repelling each other, as suggested in the original hypothesis of pyrophosphate

(19) Pauling, L. *The Nature of the Chemical Bond*; Cornell University Press: Ithaca, 1960.

(20) Saenger, W. *Principles of Nucleic Acid Structure*; Springer-Verlag: New York, 1984.

(21) O'Keefe, M.; Hyde, B. G. *Trans. Am. Crystallogr. Assoc.* **1979**, 15, 65.

Table 3. Pyrophosphate Hydrolysis Enthalpies (*ab Initio* Values Include ZPE) in the Gas Phase (kcal/mol)

	$\Delta H(\text{gas})$					
	AM1	PM3	SCF/6-31G**	MP2/6-31G**	SCF/6-311++G**	MP2/6-311++G**
$\text{H}_4\text{P}_2\text{O}_7 + \text{H}_2\text{O} \rightarrow 2\text{H}_3\text{PO}_4$	3.5	-2.0	0.0	4.4	1.7	5.4
$\text{H}_3\text{P}_2\text{O}_7^- + \text{H}_2\text{O} \rightarrow \text{H}_3\text{PO}_4 + \text{H}_2\text{PO}_4^-$	14.3	6.1	20.1	26.1	19.8	23.9
$\text{H}_2\text{P}_2\text{O}_7^{2-} + \text{H}_2\text{O} \rightarrow 2\text{H}_2\text{PO}_4^-$	-67.9	-80.2	-53.8	-48.3	-52.9	-49.0

hydrolysis, the phosphate moieties are actually attracted. It is important to emphasize that the intramolecular hydrogen bonds are likely unique to the gas-phase species. In the aqueous phase (under conditions where the phosphates would be protonated), hydrogen bonds between the hydroxyls and water molecules should be enthalpically and entropically favored.

The *ab initio* and semiempirical hydrolysis energies in Table 1 agree to within a few kilocalories per mol. However, for the multiply ionized phosphate species occurring at biological pH's, these differences become large (*vide infra*).

(b) Anionic Species. In aqueous solution at physiological pH (~7.4), orthophosphate and pyrophosphate exist largely as the deprotonated ions HPO_4^{2-} and $\text{HP}_2\text{O}_7^{3-}$. As has been widely noted in the literature, gas-phase reaction enthalpies of anionic phosphates provide little insight into the aqueous-phase reaction for two reasons. First, the repulsion between the unscreened negatively charged phosphates leads to extremely distorted pyrophosphate conformations. Second, since multiply-charged anions will spontaneously ionize in the gas phase, *ab initio* calculations of their structure and energetics are extremely suspect. These problems should be particularly acute for the di- and trianionic orthophosphates, HPO_4^{2-} and PO_4^{3-} , and the tri- and tetraanionic pyrophosphates, $\text{P}_2\text{O}_7^{4-}$ and $\text{HP}_2\text{O}_7^{3-}$, that have occupied HF molecular orbitals with positive orbital energies indicating that inclusion of plane-wave basis functions would lead to spontaneous ionization of these anions. Hence, the gas-phase wave functions and energies of these polyanions have little meaning. Such multiply-charged anions can exist in the aqueous phase because water or counterions act to neutralize the net charge. In this study we assume that the gas-phase anionic structures are accurate, but the electronic wave function will be re-optimized in the presence of the continuum solvent. The optimized PCM/*ab initio* wave functions have well-defined Fermi levels and positive ionization energies for all occupied orbitals.

In accordance with earlier studies emphasizing the need for diffuse basis functions to accurately model anionic systems, we used a large basis set with diffuse functions (6-311++G**) to optimize all protonation states of pyrophosphate and orthophosphate. The larger basis set with diffuse functions has little effect on the structure of the orthophosphate moieties, changing the P-O bond lengths by only ~0.005 Å. For the P-O-P bridge, however, the effects are more pronounced. For example in $\text{P}_2\text{O}_7^{4-}$, HF/6-31G* optimization yields a P-O bond length of 1.667 Å and a P-O-P angle of 159° compared to 1.639 Å and 180° from the HF/6-311++G** optimization. Like the neutral $\text{H}_4\text{P}_2\text{O}_7$, all of the proton-containing anionic pyrophosphates were found to have intramolecular hydrogen bonds linking the phosphate moieties.

The energetics of the gas-phase hydrolysis reactions for the mono- and dianionic species are given in Table 3. As anticipated by earlier theorists, the polyanionic pyrophosphates have large, negative hydrolysis enthalpies due to the repulsion between the negatively charged phosphate moieties. An exception to this trend is $\text{H}_3\text{P}_2\text{O}_7^-$ which is predicted to have a higher reaction enthalpy than the neutral species. This is a result of a combination of factors: the repulsion between the neutral and anionic ends of $\text{H}_3\text{P}_2\text{O}_7^-$ is not significantly greater than in the

Table 4. Components of the Polarizable Continuum Method/*ab Initio* Solvation Energies^a

molecule	total solution phase free energy (au)	electrostatic (kcal/mol)	cavitation (kcal/mol)	solvation <i>E</i> (kcal/mol)
$\text{H}_4\text{P}_2\text{O}_7$	-1209.8849	-31.2	15.0	-14.3
$\text{H}_3\text{P}_2\text{O}_7^-$	-1209.4700	-78.0	14.9	-61.3
$\text{H}_2\text{P}_2\text{O}_7^{2-}$	-1209.0436	-211.8	14.2	-195.8
$\text{HP}_2\text{O}_7^{3-}$	-1208.6085	-458.2	14.5	-441.9
$\text{P}_2\text{O}_7^{4-}$	-1208.1557	-791.9	15.0	-775.1
H_3PO_4	-643.0965	-28.2	10.5	-15.9
H_2PO_4^-	-642.6664	-85.0	10.1	-73.0
HPO_4^{2-}	-642.2242	-263.0	9.9	-251.2
PO_4^{3-}	-641.7708	-556.9	9.7	-545.4
H_2O	-76.2918	-12.1	5.0	-5.3

^a Note that the conversion from standard volume to 1 L (1.84 kcal/mol = $RT \ln(22.4/1.0)$) has been added to the total solvation energies (columns 4 and 5), and that the total free energies exclude the cavitation energy.

Table 5. Comparison of Total Solvation Energies Calculated by Three Different Methods (Energies in kcal/mol)

molecule	PCM/ <i>ab initio</i>	AM1-SM2	PM3-SM3	empirical estimates ¹
$\text{H}_4\text{P}_2\text{O}_7$	-14.3	-104.1	-59.7	NA
$\text{H}_3\text{P}_2\text{O}_7^-$	-61.3	-146.3	-96.6	-84
$\text{H}_2\text{P}_2\text{O}_7^{2-}$	-195.8	-282.2	-230.2	-134
$\text{HP}_2\text{O}_7^{3-}$	-441.9	-540.7	-471.2	-358
$\text{P}_2\text{O}_7^{4-}$	-775.1	-891.0	-806.3	-584
H_3PO_4	-15.9	-52.5	-34.5	NA
H_2PO_4^-	-73.0	-110.3	-86.3	-76
HPO_4^{2-}	-251.2	-299.9	-266.2	-299
PO_4^{3-}	-545.4	-629.2	-570.9	-637
H_2O	-5.3	-6.3	-6.3	-6.3 (expt.)

neutral species, and the H_2PO_4^- product is less able to stabilize a negative charge than the $\text{H}_3\text{P}_2\text{O}_7^-$ reactant.

(II) Aqueous-Phase Results. George et al.¹ predicted that the extremely large solvation energies for the anionic phosphates would dominate the hydrolysis reaction energies. The components of the solvation energy of each phosphate are given in Table 4. The total aqueous solvation energies calculated using all three solvation models are compared with George's empirical estimates in Table 5. As can be seen in this table there is surprising variation in the predicted solvation energies, even for the neutral and monoanionic species. The AM1-SM2 method, in particular, predicts up to 90 kcal/mol larger solvation energies than the other methods. Although experimental results must be the ultimate arbiter of these numbers, the AM1-SM2 results of -110 kcal/mol for H_2PO_4^- and -146 kcal/mol for $\text{H}_3\text{P}_2\text{O}_7^-$ are unreasonably large for monoanionic molecules. These anomalous values arise from unreasonably large atomic charges predicted for the phosphorus and oxygen atoms. These erroneous atomic charges (and solvation energies) have been seen in a series of second-row oxides.¹⁶

Although there is little experimental data available for the solvation energies for the pyro- and orthophosphates, precise results are available for the aqueous-phase acid constants (pK_a) of these compounds. *Ab initio* prediction of pK_a values is a notoriously difficult problem for several reasons. Firstly, practical basis set limitations make it extremely difficult to calculate with equal accuracy the gas-phase energies of the acid

Table 6. Gas-Phase Proton Affinities (kcal/mol)

reaction	MP2/6-311++G**	AM1	PM3	estimated gas-phase PA ¹
H ₄ P ₂ O ₇ → H ₃ P ₂ O ₇ ⁻ + H ⁺	307.3	328.0	338.2	311
H ₃ P ₂ O ₇ ⁻ → H ₂ P ₂ O ₇ ²⁻ + H ⁺	398.7	421.0	432.5	488
H ₃ PO ₄ → H ₂ PO ₄ ⁻ + H ⁺	325.8	338.8	346.3	311
H ₂ PO ₄ ⁻ → HPO ₄ ²⁻ + H ⁺	455.6	477.7	485.8	488

Table 7. Aqueous-Phase Acid Constants (pK_a Units)

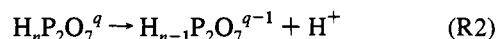
reaction	PCM/ <i>ab initio</i>	PCM/ <i>ab initio</i> (Pearson)	AM1-SM2	PM3-SM3	expt. ²⁷
H ₄ P ₂ O ₇ → H ₃ P ₂ O ₇ ⁻ + H ⁺	0.7	-4.9	13.8	25.3	0.8
H ₃ P ₂ O ₇ ⁻ → H ₂ P ₂ O ₇ ²⁻ + H ⁺	5.9	-2.0	13.3	23.5	2.2
H ₂ P ₂ O ₇ ²⁻ → HP ₂ O ₇ ³⁻ + H ⁺	10.0	5.5	10.6	32.4	6.7
HP ₂ O ₇ ³⁻ → P ₂ O ₇ ⁴⁻ + H ⁺	18.1	13.9	13.5	31.7	9.4
H ₃ PO ₄ → H ₂ PO ₄ ⁻ + H ⁺	7.7	1.3	10.3	20.2	2.1
H ₂ PO ₄ ⁻ → HPO ₄ ²⁻ + H ⁺	13.2	7.7	15.6	28.6	7.2
HPO ₄ ²⁻ → PO ₄ ³⁻ + H ⁺	18.4	11.8	14.7	34.8	12.4

Table 8. Pyrophosphate Hydrolysis Energies in the Aqueous Phase (kcal/mol)

reaction	ΔG(Aq)		
	MP2/6-311++G**	AM1-SM2	PM3-SM3
H ₄ P ₂ O ₇ + H ₂ O → 2H ₃ PO ₄	-9.3	9.6	-3.4
H ₃ P ₂ O ₇ ⁻ + H ₂ O → H ₃ PO ₄ + H ₂ PO ₄ ⁻	0.1	4.1	-11.0
H ₂ P ₂ O ₇ ²⁻ + H ₂ O → 2H ₂ PO ₄ ⁻	2.7	0.7	-12.9
HP ₂ O ₇ ³⁻ + H ₂ O → H ₂ PO ₄ ⁻ + H ₁ PO ₄ ²⁻	6.6	4.0	-21.3
P ₂ O ₇ ⁴⁻ + H ₂ O → 2HPO ₄ ²⁻	-0.8	8.2	-24.6

and its conjugate base. Secondly, accurate solvation energies are difficult to calculate. Finally, the entire range of typical pK_a values spans a range of reaction energies of about 10 kcal/mol, hence requiring extreme accuracy in all terms. Nevertheless, studies have found that within families of related compounds, systematic errors can be identified and relative pK_a values can be determined within a few pK_a units.²²

Table 6 lists the *ab initio* and semiempirical gas-phase proton affinities (PA) for the pyro- and orthophosphates, where the experimental ΔH_f for the proton of 367.2 kcal/mol was used for the AM1 and PM3 PA's.²³ The estimated PA's of George¹ are listed in the last column of this table. The predicted pK_a's are given in Table 7. The PCM/*ab initio* values are calculated from the proton transfer reaction



where the experimental solvation energy of -259.5 kcal/mol was used for the proton.²⁴ The imbalance in molecular charges between the reactants and products (neutral (or anion) + neutral → anion + cation) will lead to less accurate results. For example, the error in the free energy of the gas-phase proton transfer in water



is 29.1 kcal/mol at this level of theory. (Note that the bulk of this discrepancy arises from unusually large errors in OH⁻.)

The PCM/*ab initio* method predicts the correct ordering of the pK_a values for all the ortho- and pyrophosphates. Quantitatively, however, both the relative and absolute PCM/*ab initio* pK_a's have errors of 0-9 pK_a units, with the largest errors seen for the most highly charged species.

(22) Rashin, A. A.; Rabinowitz, J. R.; Banfelder, J. R. *J. Am. Chem. Soc.* **1990**, *112*, 4133.

(23) Stull, D. R.; Prophet, H. *JANAF Thermochemical Tables*; NSRDS-NBS 37; National Bureau of Standards: Washington, DC, 1971.

(24) Pearson, R. G. *J. Am. Chem. Soc.* **1986**, *108*, 6109.

To be consistent with the pK_a predictions of Cramer and Truhlar,¹⁵ the pK_a's were also calculated using the relation of Pearson:²⁴

$$-\Delta G_{X^-}^\circ = PA - 267 + (-\Delta G_{HX}^\circ) - 1.36(pK_a)$$

This expression yields PCM/*ab initio* pK_a's that are generally much better than those calculated directly, particularly for the orthophosphates. The errors in the relative pK_a values for the pyrophosphates from the AM1-SM2 method are actually only about ~5 pK_a units, but these results may be fortuitous since the pK_a ordering is incorrect and the AM1-SM2 orthophosphate results have much larger relative errors. (Note that our calculated pK_a's for H₃PO₄ and H₂PO₄⁻ differ marginally from those reported by Cramer and Truhlar.¹⁵)

Table 8 lists the predicted aqueous-phase hydrolysis energies using the *ab initio*-polarizable continuum model and the AM1-SM2 and PM3-SM3 methods. As expected, the aqueous solvent greatly mitigates the repulsive interactions in the anionic systems. In fact, the PCM/*ab initio* and AM1-SM2 methods predict positive hydrolysis enthalpies for almost all anionic pyrophosphates, indicating that the solvation model has overestimated the aqueous-phase stability of the pyrophosphate. The PM3-SM3 hydrolysis energies are 20-30 kcal/mol lower than those calculated with the other two methods, because PM3-SM3 overestimates the solvation energies of the pyrophosphates relative to the orthophosphates.

The experimental hydrolysis free energy for pyrophosphate is -5.1 kcal/mol at pH 7.0.² At this pH the pyrophosphates will exist primarily in trianionic and dianionic forms. The predicted hydrolysis free energy using the PCM/*ab initio* method is 6.6 kcal/mol for the prominent trianionic H₁P₂O₇³⁻ and 2.7 kcal/mol for the dianionic H₂P₂O₇²⁻. Hence, our predictions are high by as much as 12 kcal/mol. There are several sources of error in the calculation that could lead to this final error. Firstly, as mentioned above, the gas-phase HF optimizations may lead to unreliable structures and energies due to the inherent instability of polyanionic compounds in the gas phase. Sec-

only, even if the gas-phase anionic structures are reliable, they are likely to change upon aqueous solvation, an effect not yet incorporated into our solvation model. Thirdly, the predicted electrostatic solvation energy is somewhat sensitive to the details of the solvent-accessible surface. For example, using a smaller probe radius (the radius of the sphere that is "rolled" across the Van der Waal's surface) of 0.8 Å, rather than 1.4 Å, to generate the solvent accessible surface causes the predicted aqueous-phase hydrolysis energies of $\text{H}_4\text{P}_2\text{O}_7$ and $\text{H}_1\text{P}_2\text{O}_7^{3-}$ to increase to -8.7 and 7.8 kcal/mol, respectively, while the $\text{H}_2\text{P}_2\text{O}_7^{2-}$ hydrolysis energy decreases very slightly to 2.6 kcal/mol. These results will exhibit a similar sensitivity to the choice of Van der Waal's radii. Reasonable arguments can be made for a range of Van der Waal's²⁵ and probe radii,^{11,26} but it is clear that the choice of these radii will have a large effect on the results for highly charged compounds. Finally, the PCM/*ab initio* solvation model does not include dispersion terms, so that it is likely to underestimate the solvation energies.

Of the three methods employed, PM3-SM3 predicts negative free energies for all of the hydrolysis reactions shown in Table 8. Although PM3-SM3 predicts the correct sign of the reaction energy, this is likely to be fortuitous in light of the large errors in the predicted $\text{p}K_a$'s of the reactants and products. This result must be kept in mind when this method is applied to large biologically important polyphosphates such as adenosine triphosphate (ATP) which are too large to be practical for *ab initio* investigation.

Returning to the original question of whether intra- or intermolecular effects lead to the negative free energy of pyrophosphate hydrolysis, this study demonstrates that a simple answer is elusive. In the gas phase, the hydrolysis energy for the neutral $\text{H}_4\text{P}_2\text{O}_7$ is positive due to intramolecular hydrogen bonds linking the phosphate groups. For the polyanionic species in the gas phase, intramolecular repulsion overwhelms the hydrogen bonding to yield strongly negative reaction energies. In the aqueous phase, this intramolecular repulsion is mitigated by electrostatic solvent interactions. These results suggest that the most accurate overall description of the hydrolysis is that there is a delicate balance between intramolecular repulsion and the intermolecular solvent interactions.

The balance between the intra- and intermolecular effects is evident in the relation between the charge on the pyrophosphate and the aqueous-phase hydrolysis energies. The PCM/*ab initio* results in Table 8 qualitatively agree with the enthalpy results of George *et al.*,¹ who found that in the aqueous phase, neutral $\text{H}_4\text{P}_2\text{O}_7$ has a hydrolysis enthalpy 4 kcal/mol lower (more negative) than $\text{P}_2\text{O}_7^{4-}$, indicating that the solvent interaction has more than compensated for the very large intramolecular repulsion for the tetraanionic species. Note that George does not find the same trend for the free energies of hydrolysis due to an unusually high ΔS of +23 eu for the $\text{P}_2\text{O}_7^{4-}$ hydrolysis compared with -7 to $+5$ eu for the other protonation states. We predict a much more narrow range of hydrolysis entropies of (+4.2 to +11.1 eu) with the $\text{P}_2\text{O}_7^{4-}$ hydrolysis having the lowest ΔS in this range.

Conclusions

The goal of this study was to determine if the negative hydrolysis free energy of pyrophosphate is caused by intra- or

intermolecular effects. These calculations find that in the gas phase the hydrolysis of the fully-protonated pyrophosphate is unfavorable by 5 kcal/mol. The origin of this unfavorable free energy is a pair of intramolecular hydrogen bonds that link the two phosphate moieties. The H bonds have the structural effect of reducing the O-P-O bridging angle by 10 – 20° relative to earlier predicted structures.

As expected, for the anionic forms of pyrophosphate that exist near neutral pH, the gas-phase hydrolysis energies are strongly negative due to electrostatic repulsion. All of the aqueous solvation models used act to cancel this repulsion, leading to hydrolysis energies in the range -25 to $+10$ kcal/mol. The *ab initio* aqueous-phase result, which we anticipate to be most reliable, yields hydrolysis energies of 3–7 kcal/mol for the protonation states predominant near physiological pH.

Considering the large solvation energies predicted for the anionic phosphates, it is reasonable to take the view that the near-zero free energy found in most of the hydrolysis reactions is purely fortuitous. Indeed the errors in the predicted $\text{p}K_a$'s suggest that there is considerable room for continued refinement in the prediction of aqueous-phase reaction energies.

An important methodological conclusion from this study is that even for relatively small compounds in the gas phase, complete investigations of the conformational space are required, particularly in cases where intramolecular hydrogen bonding is possible. Such searches may greatly increase the computer resources needed for such studies. We also note that extreme care must be used in applying semiempirical methods to compounds containing second-row atoms, since they may produce anomalously high atomic charges.

Continuum-based solvation methods yield reasonable solvation-phase reaction energies. However, more accurate methods or carefully calibrated empirical corrections are required to achieve predictive accuracy for acid constant calculations. The complexity and subtle energetics of biochemical systems raise many challenges to their theoretical modeling. A careful analysis of the accuracy of all of the gas-phase and aqueous-phase energy terms is a necessary first step to predictive simulations of these processes.

Acknowledgment. This work was carried out in part at the Sandia National Laboratory under contract from the U.S. Department of Energy and supported by its Division of Basic Energy Sciences.

Note Added in Proof: During the final corrections to this paper, a gas-phase *ab initio* study of pyrophosphate and its anions was published that predicted the presence of intramolecular hydrogen bonding nearly identical to our findings (Ma, B.; Meredith, C.; Schaefer, H. F. *J. Phys. Chem.* **1994**, *98*, 8216).

Supplementary Material Available: HF/6-311++G** optimized structures of all ortho- and pyrophosphates, the *ab initio* and semiempirical total enthalpies and energies, and plots of the torsional potential energy surfaces for the $\text{H}_4\text{P}_2\text{O}_7$ and H_3PO_4 hydroxyl groups (6 pages). This material is contained in many libraries on microfiche, immediately follows this article in the microfilm version of the journal, can be ordered from the ACS, and can be downloaded from the Internet; see any current masthead page for ordering information and Internet access instructions.

JA941106V

(25) Marcus, Y. *Chem. Rev.* **1988**, *88*, 1475.

(26) Ooi, T.; Oobatake, M.; Némethy, G.; Scheraga, H. A. *Proc. Nat. Acad. Sci. U.S.A.* **1987**, *84*, 3086.

(27) Martell, A. E.; Smith, R. M. *Critical Stability Constants*; Plenum: New York, 1982.